Secondary-electron effects in photon-stimulated desorption

D. E. Ramaker, T. E. Madey, and R. L. Kurtz
Surface Science Division, National Bureau of Standards, Gaithersburg, Maryland 20899

H. Sambe
Chemistry Department, George Washington University, Washington, D.C. 20052

(Received 13 July 1987)

The magnitude of secondary-electron contributions to electron- or photon-stimulated desorption (ESD) or (PSD) yields is considered. In particular, we have reexamined three systems where a dominant x-ray-induced ESD (XESD) effect has been postulated. Recent ESD ion-angular-distribution data on the NH_3/Ni system and a detailed determination of the mechanisms involved in H^+ desorption indicate that all of the features previously attributed to the XESD effect may in fact arise from direct core-level processes. A reexamination of the PSD N^+ and O^+ yields from condensed N_2-O_2 reveals that the indirect XESD mechanism contributes just one-third of the N^+ yield, but dominates the O^+ desorption. This arises because the direct Auger-stimulated desorption (ASD) process following core-hole excitation is inactive for O^+ desorption, but remains active for N^+. Finally, a detailed interpretation of H^+ desorption from OH/Ti and OH/Cr, and comparison with the system OH/YbO-Sm indicates that the direct ASD process is also inactive in the latter case. This investigation concludes that in cases for which the direct ASD process is active, the indirect XESD contribution is generally on the order of 35% or less. When the ASD process is suppressed, the XESD process generally dominates. However, in chemisorbed systems, even when the direct process is relatively inactive, the XESD process does not dominate. The various reasons for this are discussed.

I. INTRODUCTION

Recent reports on the extent of secondary-electron contributions in electron- or photon-stimulated desorption (ESD or PSD) appear to be contradictory. Jaeger *et al.*[1] suggested that secondary electrons provide the dominant contribution to the H^+ yield from NH_3/Ni and called the process x-ray-induced ESD (XESD). Others have concluded that the XESD process is the dominant mechanism in the PSD of N^+ and O^+ ions from mixed condensed gases such as N_2-O_2 (Ref. 2), and in the PSD of H^+ ions from OH/YbO-Sm (Ref. 3). On the other hand, considerable evidence exists in the literature for the dominance of direct photon excitation mechanisms. This includes the following.

(a) Large differences were found in the photon-energy dependence between the secondary-electron yield and the PSD O^+ yield from O/Cr (Ref. 4), O/W (Ref. 5), and $NaWO_3$ (Ref. 6).

(b) Similar differences were found for the PSD of H^+ ions from OH/Ti and OH/Cr (Ref. 7), and from H_2O/SiO_2 (Ref. 8).

(c) A comparison of the ESD O^+ yield from NO/Pt (110) (Ref. 9), originating from molecularly adsorbed NO, revealed that the threshold energy for O^+ desorption is at the O *K* level.

(d) The PSD O^+ yield from CO/Ru(0001) shows no structure at the Ru core levels.[10]

(e) The PSD H^+ yield from diamond is large in the valence-energy region but relatively small in the core-level region.[11] Furthermore, comparison of the core-level PSD H^+ yield from the diamond surface with the C 1*s* constant-initial-state (CIS) photoemission spectrum reveals significant differences, namely the absence of the excitonic feature in the H^+ yield.[11]

(f) A semiquantitative determination of the secondary-electron contribution to the ESD OH* yield from OH/TiO_2 indicated that backscattered electrons were responsible for only about 30% of the OH* desorption.[12] This is true even though the OH* yield has a sharp threshold already at 11 eV (relative to the Fermi level) where large secondary-electron densities are expected. The situation in ESD and PSD should not be that much different.

We note that the magnitude of the XESD process in PSD is an extremely important question. The mechanisms for stimulated desorption are complex and varied, often involving many-body excited intermediate states [e.g., two-hole ($2h$), two-hole–one-electron ($2h$-$1e$), and others ($2h$-$2e$, $1h$-$2e$, etc.)].[13,14] Most helpful in sorting out these varied mechanisms has been the comparison of the photon-energy dependence of the ion spectral yield with constant-initial-state photoelectron spectra or secondary-electron yields, both of which generally reflect the total absorption coefficient.[15] This comparison, along with identification of the features in the excitation spectrum, allows us to determine which excitations lead to desorption and which do not. If, however, the ion yield is dominated by effects from the secondary and backscattered electrons, then this comparison provides no information because the ion yield will simply reflect the bulk density of states (DOS), regardless of the excitation involved.

In some ionic systems, in which the direct process may not be very selective as to the active final states, the ion

yield may reflect the final DOS at the outermost surface layer, information which is normally of great interest but often difficult to obtain.[16] Moreover, in these cases, PSD extended x-ray-absorption fine-structure measurements well above the substrate absorption edge suggest the possibility for determination of the surface structure.[17(a)] The presence of XESD contributions and the often limited selectivity among the final states of the direct desorption process makes this prospect highly limited however.

In this paper we will reexamine the three systems mentioned above where a dominant XESD effect has been postulated. We will show for these three systems that either alternate interpretations of the data are possible, indicating that the XESD effect is small, or that the XESD process dominates only because the direct mechanism is suppressed. This makes the results on these three systems consistent with the significantly larger number of papers which indicates that the XESD effect is generally not a major cause of ion desorption.

II. SYSTEMS STUDIED

A. NH_3 on Ni(110)

The H^+-yield data from NH_3/Ni(110), as reported by Jaeger *et al.*,[1] appears to provide convincing evidence that the XESD process is predominant. Figures 1 and 2 reproduce their data at the Ni L and N K edges. They compare the total electron yield (TEY) with the H^+ PSD

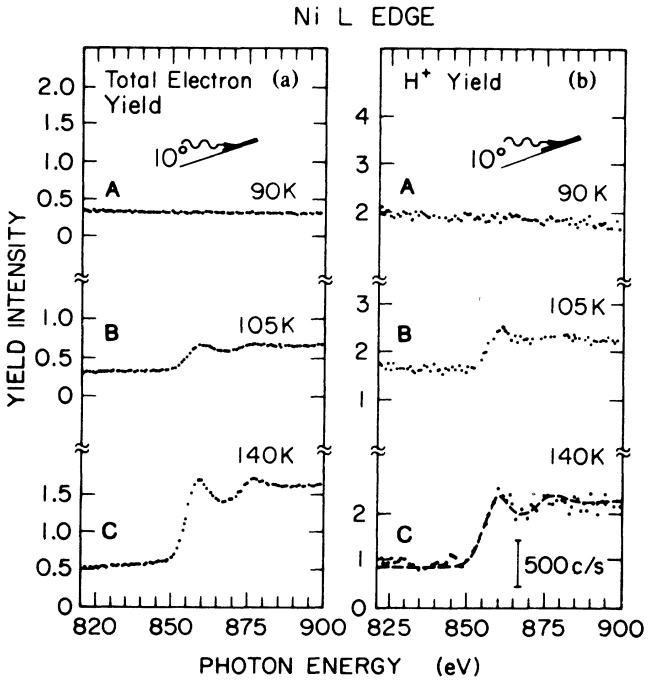

FIG. 1. Data reported by Jaeger and Stöhr (Ref. 1) showing (a) the total electron yield and (b) the H^+-ion yield from NH_3/Ni near the Ni L edge. The data were taken after stepwise annealing of a saturated NH_3 multilayer on Ni(110), prepared at 90 K, to the listed temperatures for 60 s each. Total electron yield is indicated in arbitrary units; H^+ yield in units of 500 counts/s.

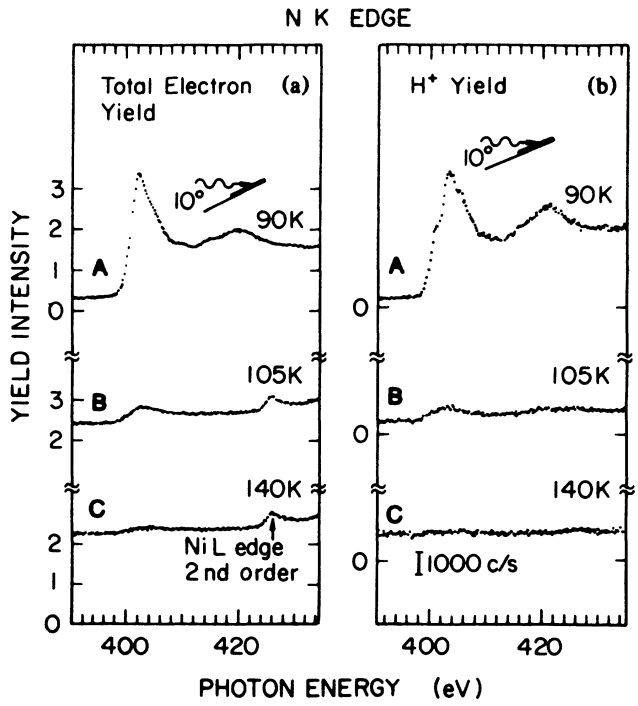

FIG. 2. Data reported by Jaeger and Stöhr (Ref. 1) showing (a) the total electron yield and (b) the H^+ yield from NH_3/Ni near the Ni K edge. The data were taken on samples prepared similarly to those in Fig. 1. Total electron yield is indicated in arbitrary units; H^+ yield in units of 1000 counts/s.

yield as the NH_3 coverage is changed by careful annealing from 90 to 140 K. Electron emission and ion desorption at the Ni L edge are absent at 90 K because the NH_3 layer thickness considerably exceeds the electron escape depth. At 105 K, where the NH_3 layer was believed to still have an appreciable thickness, the Ni L edge becomes visible in the H^+ yield. Thus Jaeger *et al.* concluded that their H^+ desorption was dominated by the indirect XESD mechanism, since the Ni atoms were believed to be separated by many NH_3 layers from the outer surface. Figure 2 shows that at the N K edge the TEY and H^+ yields are very similar, except for the presence of a shoulder in the H^+ yield at 400.5 eV which is not present in the TEY. This shoulder (and a proportional amount of the spectrum at higher energies) was interpreted by Jaeger *et al.* to arise from the direct core-level excitation of a surface NH_3 molecule, the remainder of the yield spectrum arising from the XESD process. Based on this interpretation, the XESD process is estimated to cause 60% of the total yield.

The conclusions based on measurements at the Ni L edge depend critically on the actual coverage maintained at each temperature. At the Ni L edge (Fig. 1), Jaeger *et al.*[1] observed a H^+ signal after annealing 60 s at 105 K, so that the "outermost NH_3 layer is separated from the Ni substrate by many intermediate layers." However, the vapor pressure of NH_3 at 105 K is $\sim 3\times 10^{-6}$ Torr,[17(b)] and the evaporation rate is high enough (several monolayers per second) that *all multilayers of NH_3 are probably absent.* Based on thermal desorption studies of

NH_3/Ni(110), the coverage of molecular NH_3 stable at 105 K is, at most, two molecular layers, with a total coverage of $\sim 8\times 10^{14}$ molecules/cm^2.[18] The second NH_3 layer (the β state[18]) is more tightly bound than multilayer NH_3 probably because it *does interact* weakly with the Ni(110) substrate. Thus, the observation of H^+ at the Ni L edge may be due mainly to Auger-stimulated desorption, just as for H^+ from OH on Cr and Ti.[7]

We suggest that the thicknesses of the NH_3 films used by Jaeger *et al.*[1] were considerably different from those reported. As indicated above, the "thin" film at 105 K was probably much thinner than reported, ~ 2 layers at most. The "thick" film at 90 K was probably much thicker (maybe even 2–3 times thicker) than the 16 layers they reported, in order for the TEY to be suppressed completely at the Ni L edge, as shown in Fig. 1.

To settle the issue of direct versus indirect excitation at the Ni L edge, the following experiment should be done using careful, quantitative dosing of NH_3.[19] Deposition of three or four molecular layers of NH_3 at 80 K should mask the NH_3-substrate interaction, assuming layer-by-layer growth. If the direct mechanism dominates, the H^+ signal should be absent at the Ni L edge. If the indirect XESD mechanism is operative, the H^+ yield should be observable and should persist to much thicker films.

Jaeger *et al.*[1] also presented data demonstrating, at the N K edge, the linearity between the increase in the H^+ yield, ΔI_{H^+}, and the incremental change in TEY, ΔI_{TEY}. This linearity was used to support the indirect XESD mechanism at the N K edge. We suggest that this apparent linear behavior may be a consequence of a limited data set. For NH_3 deposited onto metals[18] and studied using ESD, ΔI_{H^+} is strongly nonlinear as a function of NH_3 coverage in the range 0–5 molecular layers: this is due both to reneutralization effects and to molecular orientation effects. For the first layer in contact with Ni(110), the angular distribution of the ion desorption is in the form of a "halo" of H^+ emission, and no H^+ desorbs normal to the surface.[18] As subsequent layers form, the H^+ emission is dominated by desorption centered around the surface normal. On the other hand, ΔI_{TEY} is expected to be more nearly linear with increasing NH_3 coverage. When ΔI_{H^+} is plotted versus ΔI_{TEY}, the resultant curve should resemble the nonlinear plots of ΔI_{H^+} versus NH_3 thickness.[18] In fact a nonlinear (s-shaped) curve can be fitted to the data points of fig. 3 in Ref. 1. To summarize: the ESD H^+ yield saturates at 5–6 molecular layers, whereas the TEY should continue to increase up to much higher film thicknesses. The way to clarify the roles of secondary electrons in PSD of NH_3 at the N K edge is to measure both ΔI_{H^+} and ΔI_{TEY} quantitatively as a function of film thickness.

The shoulder in the H^+ yield from condensed NH_3 at 400.5 eV near the N K edge [Fig. 1(b), A] is comparable to that seen in the D^+ yield from condensed D_2O at 534 eV near the O K edge.[20] Indeed, over a 40-eV region above the respective K edges, the D^+ yield from D_2O is similar to that for H^+ from NH_3/Ni. These are clearly due to direct excitations since there are no corresponding features in the TEY curves. A detailed interpretation of the D^+ yield indicates that the shoulder arises from the $1a_1^{-1}4a_1$ excitation, which has a higher branching ratio for subsequent H^+ desorption than $1a_1^{-1}R$ or $1a_1^{-1}kl$ excitations.[21] (Here the $4a_1$ orbital is a highly antibonding valence orbital appearing just below the vacuum level. R and kl indicate the Rydberg and continuum orbitals and $1a_1$ is molecular-orbital notation for the O 1s level.) The most probable decay of these core excited states occurs through an Auger process leaving two valence holes (v^{-2}); hence $1a_1^{-1}4a_1 \rightarrow v^{-2}4a_1$, $1a_1^{-1}R \rightarrow v^{-2}R$, and $1a^{-1}kl \rightarrow v^{-2}$ (the continuum electron also leaves the vicinity of the core hole). Because of the antibonding character of the $4a_1$ orbital, its occupation encourages OH bond breaking and increases the probability for desorption from the $1a_1^{-1}4a_1$ core state. Similar arguments also accounted for the increased peak in the D^+ yield relative to that in the TEY at 20 eV above the O K level.[21] Examination of the H^+ yield in Fig. 2 also indicates that the H^+ yield has a more pronounced peak at 421 eV compared to the peak in the TEY spectrum. Thus the difference in the TEY and H^+ yield spectra reflect important final state effects and argue against a large XESD effect.

Jaeger *et al.*[1] also assign the $1s^{-1}4a_1$ excitation to the shoulder at 400.5 eV: they conclude that the $1a^{-1}4a_1$ excitation has large probability only at the NH_3 surface, while the $1a^{-1}3p$ excitation dominates in the NH_3 bulk. However, this conclusion is not necessary to explain the data, as we indicate above.

We note that recently Rehn and Rosenberg[2(b)] also examined the data of Jaeger *et al.*[1] They concluded that "the lack of morphological measurements and direct thickness measurements in the data weakens the evidence for XESD." Although their conclusions regarding the role of the XESD process in this system are similar to ours, they interpret the PSD data near the N K edge very differently from the interpretation given above. They indicate that the shoulder in the H^+ PSD yield at the N K edge is due to two different NH_3 sites in the layer, namely, the Ni-NH_3 site and the NH_3-NH_3 site, the latter site being more characteristic of the thick film. The presence of the Ni-NH_3 site feature even for the thick layers then suggests to Rehn and Rosenberg that the film morphology was varying or that "snowflake or island structure" existed in the layer. Although we cannot rule out such structure, the presence of a similar shoulder in the D^+ yield from thick D_2O films,[20] which are known to be well-ordered films, suggests that the shoulder in the H^+ yield from NH_3 does not come from the two different sites, but from the different branching ratios as we proposed above.

B. Mixed condensed O_2 and N_2

Recent data by Parks *et al.*[2] for the PSD of N^+ and O^+ from the surface of a condensed mixture of N_2 and O_2 has provided additional evidence for the importance of the XESD process. Figure 3 shows the TEY and O^+

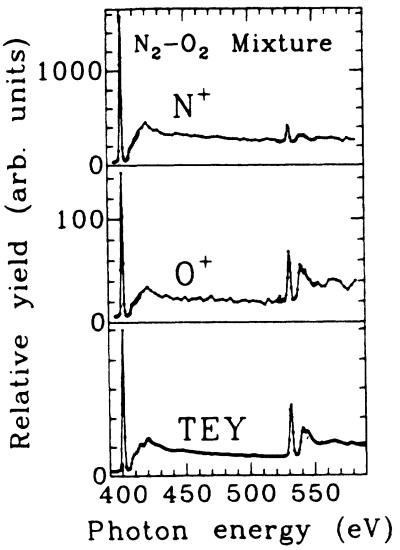

FIG. 3. Data reported by Parks *et al.* (Ref. 2) showing the N^+, O^+, and the total electron yield (TEY) from a condensed mixture of N^+ and O^+ near the N and O K levels.

and N^+ yields with photon energy in the N and O K core-level energy regions. The presence of large N^+ and O^+ yields at *both* the N and O K levels indicates very strongly that indirect mechanisms are playing an important role.

Parks[2(a)] assumed that the indirect mechanisms are dominated by the normal indirect XESD process. Rehn and Rosenberg[2(b)] propose a new related indirect mechanism involving the photoelectron-stimulated dissociation (i.e., XESD) of surface molecular ions. In this mechanism, molecular ions resulting from surface charging are dissociated by low-energy electron impact. Both groups analyzed the data on the basis of X^+ ions desorbed per surface $1s_y$ core-level excitation.

In the analysis by Parks *et al.*,[2] the quantity $I(X^+,1s_y)$ is obtained from the simple expression $I(X^+,1s_y)=N_x f_y \sigma_y c$. Here N_x is the experimental X^+ ion yield (ions/s), f_y is the experimental photon flux (photons/s cm^2) in the region of the $1s_y$ core level, σ_y is the $1s_y$ core-level photoionization cross section (cm^2/layer),[23–25] and c is the concentration of molecules per layer (assumed by Parks *et al.* to be 10^{15} molecules/cm^2 layer). On the basis of the data, they obtained the results, $I(N^+,1s_N)=1.1\times10^{-3}$, $I(O^+,1s_N)=8.1\times10^{-5}$, $I(N^+,1s_O)=1.6\times10^{-3}$, and $I(O^+,1s_O)=6.6\times10^{-3}$. They also took the reasonable viewpoint that the X^+ desorbing at the $1s_y$ edge results from the indirect XESD mechanism, while the X^+ desorbing at the $1s_x$ edge results from a combination of direct and XESD mechanisms. Thus from the results above, one concludes that the N^+ yield via the XESD mechanism dominates by a factor of 2.5 over the total O^+ yield at the $1s_O$ edge, but at the $1s_N$ edge the O^+ XESD yield is only 10% of the total N^+ yield. They concluded that the XESD mechanism predominates for N^+, but is small for O^+ desorption from the N_2-O_2 mixture.

Their analysis places a heavy reliance on estimates of absolute quantities, namely, on their experimental absolute ion yields and photon fluxes, and on previously reported photoionization cross sections. The latter, in particular, are not known very accurately; estimates for O_2 differ by over a factor of 4 and errors here alone could substantially affect their conclusions. We prefer to rely on the total electron yield as reported by Parks *et al.* and shown in Fig. 3. Indeed, a simple comparison of the O^+ and N^+ yields with the TEY reveals that the O^+ yield is very similar to the TEY, while the N^+ is very different. This immediately suggests the opposite from their conclusions, namely, that the O^+ yield is dominated by the indirect XESD mechanism, while the N^+ yield is not.

In the Appendix we present a detailed theoretical analysis of the data from Parks *et al.*[2] It utilizes the TEY data and avoids the necessity for knowledge of absolute quantities. It utilizes only relative quantities, indeed photon-independent relative quantities to the extent possible. We also use some recent PSD data of Rosenberg *et al.*[26] on the pure O_2 and N_2 condensed gases. Our final conclusions are consistent with those obtained from a simple comparison of the ion yields with the TEY as indicated above, and the opposite from the conclusions reached by Parks *et al.*[2]

We conclude that the XESD indirect channel has just a 30–40 % effect on the N^+ desorption, but dominates the O^+ desorption. We will further indicate below that the dominance of the XESD effect for O^+ desorption arises because the direct Auger-stimulated (Coulomb explosion) desorption (ASD) mechanism, normally active in gas-phase diatomics such as O_2, N_2, and CO,[13,22,26,27] is nearly inactive in condensed O_2 (also in NO). The indirect mechanism dominates, of course, when the direct mechanism is suppressed.

1. Results and discussion

Let us summarize our results from the Appendix in detail and discuss them in sequence. We have found the following.

(1) The secondary-electron yields for the pure substances (condensed O_2 and N_2) are nearly equal.

(2) The relative surface concentration of $[N_2]_s/[O_2]_s=1.1$ is comparable to that in the bulk $[N_2]_b/[O_2]_b=1.35$.

(3) The ratio of the XESD cross sections in pure N_2 and O_2 is of the order one, i.e., 1.5.

(4) The ratio of the direct PSD cross sections in N_2 and O_2 is very different from one, i.e., 20.

The similar secondary-electron yields for N_2 and O_2 reflect either similar $1s$ photoabsorption cross sections for N_2 and O_2, or a compromising effect due to the higher $1s$ binding energy of O_2. The photoabsorption cross section $1s\rightarrow6\sigma^*$ for N_2 has been estimated to be 2.3×10^{-18} cm^2; estimates range from 0.5 to 2.1×10^{-18} cm^2 for O_2.[23–25] If the smaller estimate for O_2 is correct, then the subsequent Auger-decay and extrinsic loss processes must result in a greater number of secondary electrons per excitation to give the same total yield. On the other hand, the smaller nitrogen-to-oxygen absorption cross section

ratio, $2.3/2.1=1.1$, is remarkably close to the yield ratio $[N]/[O]=1.06$, making the larger estimate for the O_2 cross section more consistent with the PSD data (Parks *et al.*[2] used the smaller estimate for O_2, and we believe this is the primary reason for their different conclusions).

Our analysis allowed for the relative surface concentration, $[N_2]_s/[O_2]_s$, to be different from the bulk concentration, $[N_2]_b/[O_2]_b=1.35$, since we expected that either segregation to the surface from the bulk or a thermodynamic condensation effect at the surface might be possible. Surface segregation is well known in transition-metal alloys, which are also weakly bonded.[28,29] Another possibility is that the larger heat of evaporation for O_2 (6.8 kJ/mol versus 5.7 kJ/mol for N_2) (Ref. 30) and lower melting point for O_2 (54 K versus 62 K for N_2) (Ref. 31) might make the O_2 condensation coefficient lower than that for N_2 at the surface. Our result of $[N_2]_s/[O_2]_s=1.1$ is within the experimental error of the bulk mixture, suggesting that neither possibility is occurring to a great extent. This may arise because of the precautions taken by Parks *et al.*,[2] who condensed the N_2-O_2 mixture on a liquid-He-cooled aluminum substrate in ultrahigh vacuum (UHV), and continually refreshed the surface by slow condensation of vapor from a doser tube when the data were taken. Nevertheless, we believe that different concentrations at the surface and in the bulk generally may exist in condensed molecular mixtures, and precautions should be taken when attempting to perform quantitative surface sensitive studies.

The indirect cross sections can be related to the direct dissociation yields in the gas phase[32] and desorption from the condensed phase,[20] particularly those resulting from photon or electron excitation energies in the valence region (0–35 eV), i.e., the energy where most of the secondary electrons appear. The data are summarized in Table I. The O^+ yield is much larger than the N^+ yield for the gas phase in this energy region; however, in the condensed phase they are comparable. The dissociation of O_2 and N_2 in the gas phase has been studied extensively.[33–36] It is known that the dominant dissociation mechanism in O_2 proceeds via predissociation of several one-hole ($1h$) states, which have rather long lifetimes in spite of this decay mechanism.[35] These slow dissociation mechanisms are not expected to occur in the solid phase because of other energy-delocalization mechanisms, and apparently this indeed is true as suggested by the significant reduction in the O^+ yield upon condensation (Table I). The N_2 dissociation, like CO dissociation, primarily proceeds directly from repulsive two-hole–one-electron ($2h$-$1e$) states and these are expected to remain active in the condensed phase.[13] These $2h$-$1e$ mechanisms are also present in O_2, but are insignificant compared to the $1h$ predissociation processes in the gas phase.[33–36] Upon condensation only the $2h$-$1e$ processes remain in O_2, and the atomic ion yields in N_2 and O_2 become comparable. This is suggested both by the PSD yields in the region 17–35 eV and by our indirect yield [N]/[O] ratio, obtained above.

TABLE I. Comparison of reported ion yields produced at core and valence levels in the condensed and gas phase for N_2, CO, NO, O_2, and N_2O.

Molecule	Ion	Molecule[a] (K level) condensed	σ per atom[b] (K level) condensed	Max ions per $h\nu$[c] valence condensed	$[X^+]/[X_2^+]$, average[d] valence gas phase
N_2	N^+	44 (N)	22 (N)	1.6	0.02
	N_2^+	0.96 (N)	0.5 (N)	0.5	
CO	C^+	20 (C)	20 (C)	1.6	0.03
		36 (O)	36 (O)		
	O^+	4.9 (C)	4.9 (C)	0.06	0.002
		9.5 (O)	9.5 (O)		
	CO^+			0.06	
NO	N^+	3 (N)	3 (N)	0.2	0.04
		1.5 (O)	1.5 (O)		
	O^+	0.9 (N)	0.9 (N)		0.005
		1.8 (O)	1.8 (O)		
	NO^+	2.1 (N)	2.1 (N)	0.4	
		4.4 (O)	4.4 (O)		
O_2	O^+	14 (O)	7 (O)	2	0.11
	O_2^+	4.1 (O)	2.0 (O)	0.02	
N_2O	N^+	2.6 (N)	1.3 (N)	2	0.4 (0)
	O^+	2.5 (N)	1.2 (N)	0.6	0.2 (0.07)
	NO^+	12 (N)	6 (N)	2	0.50 (0.10)
	N_2^+			1	0.13 (0)

[a]σ in units of 10^{-22} cm^2/eV mol at either the N K (422 eV), C K (296 eV), or O K ($\sim$553 eV) levels as reported by Rosenberg *et al.* (Ref. 26).

[b]Data in column 1 divided by number of N, C, or O atoms in each molecule.

[c]Maximum ion yield (10^{-8} ions/photon) in the region $h\nu=14$–35 eV from condensed solids as reported by Rosenberg *et al.* (Ref. 20).

[d]Average yield $[X^+]/[X_2^+]$ in the region $h\nu=17$–35 eV, as obtained in the gas phase. Data for N_2O from Ref. 56 at $h\nu=21.2$ eV, that in parentheses at 17.1 eV from Ref. 56. All other data from Ref. 32.

Finally, the direct yield ratio, $[N]/[O]=20$, indicates that the dissociation process at the $1s$ core level is nearly inactive in O_2. The primary core-level dissociation process in diatomics involves Auger decay of the core hole, resulting in a two-hole ($2h$) final state, which directly results in dissociation via a "Coulomb explosion."[22,27] The direct ASD model is known to be active in the gas phase,[22,27] and it is believed to be active also in the condensed phase, at least for N_2 and CO.[26] It is known, however, that upon chemisorption on metals this process at the K edge is terminated due to electron transfer from the metal substrate into the $2\pi^*$ orbital.[15] This transferred electron screens the two valence holes caused by the Auger decay and thus prevents the Coulomb explosion. Some desorption still remains at energies well above the K edge, but this arises due to a core-hole–plus–shake-up mechanism resulting in $3h$-$1e$ or $3h$-$2e$ final states, which are repulsive and directly lead to desorption.[15] These many-particle (nh-me) processes also occur in the gas phase, but are negligible compared to the $2h$ ASD processes in this case.

We believe that a similar charge-transfer termination process is occurring in the condensed O_2-N_2 mixture, only in this case the charge transfer occurs from a resonant $2\pi^*$ orbital of a neighboring O_2 molecule. This process cannot occur in condensed N_2 because the $\pi_u 2p$, the comparable $2\pi^*$ orbital, is empty.

Evidence that this electron-transfer process can occur in O_2 comes from visible-absorption spectra. Isolated O_2 dimers in a solid neon host have a characteristic absorption spectrum[37] resulting from absorption of a single photon at 6300 Å to produce a singlet state in which both halves of the dimer are electronically excited, $^3\Sigma_g^+ + {}^3\Sigma_g^+ \rightarrow {}^1\Delta_g + {}^1\Delta_g$. Both the electronic energy transfer and singlet-triplet splitting in the dimer ground state are believed to result from electron exchange of the $2\pi^*$ electrons. The growth of larger clusters causes the unique dimer spectra to disappear.[37] The α phase of O_2, which exists below 24 K, is antiferromagnetically ordered.[38–40] Bimolecular absorption lines also appear in this case, but the spectrum is significantly broadened and shifted. The spectrum in α-O_2 is explained by taking into account the collective nature of the excited crystal states.[41] It is found, however, that by either raising the temperature above 24 K, which produces the β phase, or by introducing small amounts of N_2, the antiferromagnetic ordering is disrupted and a spectrum resembling the isolated dimer spectrum appears.[42] Thus the N_2-O_2 condensed mixture may have a significant proportion of O_2 dimers, particularly at the surface where the antiferromagnetic ordering is the most easily disrupted.

On the other hand, recent absorption and photoelectron data on condensed N_2 and O_2 reveal that the $2\pi^*$ band is significantly broadened by normal intermolecular interaction.[43,44] This would suggest that $2\pi^*$-electron exchange may occur even in the absence of dimer formation. We will give evidence below that even in pure O_2 the direct ASD process is inactive. It is possible that it is decreased in the mixed N_2-O_2 solid because of increased dimerization, but dimerization may not even be necessary.

2. *Comparison with other systems*

Direct evidence has been given recently that $2\pi^*$ electron transfer does occur in condensed NO.[45] Valence and core photoelectron spectra show satellite features attributed to intermolecularly screened and unscreened core- and valence-hole states. NO is known to dimerize as ON-NO in the solid, and theoretical calculations show that the $2\pi^*$ orbital has a strong N-N overlap when one of the N atoms has a core hole.[45–47] In contrast, for an O core hole in NO, very little charge transfer is evident in both experimental data and theoretical calculations.[45–47]

The discussion above for pure NO and O_2 suggests that the direct ASD process is relatively inactive in both of these systems. Comparison of yield data[26] given in Table I for NO and O_2 with that for pure CO and N_2, where it should be active, indicates that this appears to be the case. Note that the total atomic ion cross section per atom at the K edges in units of 10^{-22} cm^2/atom is in the range 3–7 for NO and O_2, but in the range 22–70 for CO and N_2. Note, however, that the parent ion (X_2^+) generally ranges from 2–4 for O_2 and NO, while it is about 0.5 or less for CO and N_2. The larger parent-ion yields for O_2 and NO probably result from the screened $2h$ states which do not result in a Coulomb explosion.

Further evidence for the inactivity of the ASD mechanism in NO and O_2 comes from comparison of the ion-yield spectra with the TEY as a function of $h\nu$, as reported by Rosenberg.[26] The O^+-yield spectra for NO and O_2 are very similar to the TEY spectra, while for CO and N_2 the peak resulting from the $1s \rightarrow 2\pi^*$ excitation is a factor of 2–4 smaller in the ion-yield spectrum than in the TEY spectrum. This occurs because the $1s^{-1}2\pi^*$ state can Auger decay as follows:[15]

$$1s^{-1}2\pi^* \rightarrow v^{-1} ,$$
$$1s^{-1}2\pi^* \rightarrow v^{-2}2\pi^* ,$$
$$1s^{-1}2\pi^* \rightarrow v^{-2} ,$$

where the $2\pi^*$ does or does not participate, or escapes via shakeoff, respectively, in the Auger decay. Only the last case results in a Coulomb explosion, and thus the $1s \rightarrow 2\pi^*$ has a reduced amplitude in the ion yield when the direct process dominates.[15] Of course, when the indirect process dominates, as proposed for NO and O_2, no difference is expected.

We should note here that there is some evidence for a direct ASD contribution to the ion yields in NO. The $[N^+]/[O^+]$ yield ratio at the N and O K levels should be the same if only the XESD mechanism is active, since the source of the electrons, the N or O K level, should not matter. (The NO^+ yield will be different because it has a direct core-level contribution.) The data indicate $[N^+]/[O^+]=3$ at the N K and 0.83 at the O K level.[26] This could mean that a direct N^+ contribution occurs at the N K level and/or a direct O^+ contribution occurs at the O K level. Since most of the valence $1h$ and $2h$-$1e$ states produce N^+ ions, as indicated by the gas-phase data[32] (i.e., $[N^+]/[NO^+]=0.04$ while $[O^+]/[NO^+]=0.005$ in Table I), the latter alternative appears more

reasonable. Although the maximum desorption yield in the valence region ($h\nu = 14-35$ eV) from the condensed phase indicates more O^+ than N^+ (see Table I),[32] the XESD contribution arises from a wide range of electron energies, so that the integral or average yield over the valence region is a more appropriate measure of the indirect XESD yield. A small direct ASD contribution to the O^+ yield from NO is also not unexpected since, as discussed above, very little charge transfer occurs upon O core-hole excitation in ON-NO. On this assumption, comparison of the $[N^+]/[O^+]$ ratios at the N K and O K levels suggest a direct ASD O^+ contribution of ~ 1.3, and 0.5 O^+ and 1.5 N^+ indirect contributions at the O K level (see Table I). The relative indirect to direct O^+ yield is then $\sim 35\%$ at the O K level, consistent with that found for N^+ from N_2 and OH^* from OH/TiO_2 when the direct process is active.[12] A careful analysis of the $2\pi^*$ peaks in the N^+- and O^+-ion yields and the TEY spectrum by Rosenberg *et al.*[26] suggests a small direct ASD contribution also occurs at the N K level, but the data for two separate runs were very different, and the statistical significance was poor. Based on our arguments above, we doubt whether a significant direct ASD contribution appears at the N K level in NO. The O_2 dimer is rectangular (D_{4h} symmetry) with all four O atoms equivalent (in α-O_2 all O atoms are equivalent);[37] thus a significant ASD contribution is not expected in O_2 either.

Table I also presents results for the triatomic N_2O molecule.[26] The total dissociated ion yield at the N K level is comparable to that for NO, suggesting that the direct ASD contribution is also small here. N_2O is a filled-shell system; however, an empty π^* orbital does lie just above the highest filled π orbital.[48-50] This could mean that dimerization or at least electron transfer also occurs in condensed N_2O. Studies of matrix-isolated N_2O dimers have been reported.[51,52] Evidence for intermolecular interaction between the lowest unoccupied π^* orbitals in isoelectronic solid CO_2 has recently been reported from absorption spectra.[53,54] The $[NO^+]:[O^+]:[N^+]$ yield ratios,[26] obtained at $h\nu = 426$ eV in the condensed phase, are 4.6:0.92:1. These are very different from those obtained at $h\nu = 423$ eV in the gas phase,[55] 0.18:0.5:1.6, but are comparable to those obtained in the gas phase between 14 and 35 eV,[56] 2.5:1.4:1.6. Thus the evidence suggests that the XESD process may also be dominant here, even for a filled-shell system, but further work is required before firm conclusions can be reached, particularly since the dissociative process in these triatomic molecules can be very complex.[57]

C. H^+ from OH/YbO-Sm

Recent reports by Schmidt-May *et al.*[3] of H^+ desorption from a metal system, which consisted of oxidized Yb on bulk Sm metal, also provide evidence for the dominance of the XESD effect. Figure 4 shows a comparison of the H^+ yield with the constant-final-state (CFS) photoelectron spectrum on this system. The large features at $h\nu = 135-160$ eV arise from the Sm $4d$-$4f$ giant resonance, that at 180–190 eV from the Yb $4d$-$4f$ resonance. Observations of the surface and bulk emissions indicate that the oxidized Yb has covered the Sm surface, so that

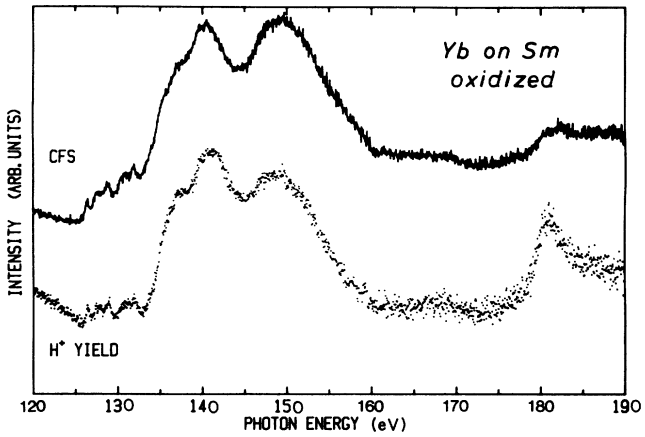

FIG. 4. Data reported by Schmidt-May *et al.* (Ref. 3) showing a comparison of the electron and H^+ ion yields from an oxidized Yb/Sm sample in the region of the $4d \rightarrow 4f$ resonance.

little if any Sm surface is thought to be exposed. In spite of this, the Sm core-level excitation produces a larger H^+ signal than the Yb excitation.[3] If indeed the Sm surface is totally covered, this strongly indicates that the XESD process is dominant in this system.

Although the source of the H atoms has not been well characterized, the H^+ which desorbs is most likely bonded to the O atoms in the oxidized Yb. The "giant resonance," $4d^{-1}4f^{n+1}$, Auger decays or autoionizes predominantly to $4f^{n-1}$, a $1h$ valence state which does not lead to desorption. Thus the direct ASD process is inactive at both the Yb and Sm core levels.[3] This situation is similar to our previous work involving OH/Ti and OH/Cr, where the $3p^{-1}3d^{n+1}$ resonance was involved.[7] In this case, the Auger-decay process led to the final states $3d^{n-1}$, v^{-1}, and $v^{-2}3d^{n+1}$ (v indicates M-OH bonding orbitals), the latter state leading to desorption. As the number of d electrons, n, increases, the branching ratio for $v^{-2}3d^{n+1}$ decreases relative to $3d^{n-1}$, in turn decreasing the H^+ yield. It follows that OH/Cr gave a lower H^+ yield than OH/Ti. In Yb and Sm, the number of f electrons is large, between 5 and 13, so that the branching ratio to the $v^{-2}4f^{n+1}$ state, which might lead to direct H^+ desorption, is very small.

Studies of H^+ desorption from OH/Ti and OH/Cr and on bulk solid H_2O indicate the dominant desorption mechanism for H^+ involves $2h$-$1e$ and $2h$ states arising from ionization plus shakeup or shakeoff.[21] These states appear around 20–45 eV in H_2O, a region rich in secondary electrons. Thus for H^+ from OH/YbO-Sm, the indirect XESD yield should be large and the direct ASD yield small, explaining the assumed (i.e., assuming the Sm surface is totally covered by YbO) dominance of the XESD effect.

III. GENERAL DISCUSSION

We have shown for the three systems discussed above that either alternate interpretations of the data are possible, indicating that the XESD effect is not dominant (but rather around 35%), or that the XESD process dom-

inates only because the direct Auger mechanism is suppressed. This makes the results on these three systems consistent with the significantly larger number of papers (as summarized in the Introduction), which indicate that the XESD effect is generally not dominant. On the other hand, the nearly complete absence of ion-yield contributions below the O K core levels from NO/Pt(110) and CO/Ru(0001) seems to be in conflict with the above.[9,10] One might have anticipated an XESD effect to produce a measurable O^+ yield below the O K level in each of these cases. Furthermore, the onset of the ion yield well above the O K level[9] appears in conflict with the data from condensed molecular gases, where we indicated that the direct ASD contribution is suppressed.

Figure 5 shows the ESD O^+ and N^+ yields for CO, NO, or N_2 on W, Ni, or Ru.[58] Although the O^+ yield for CO/W(100) shows an appreciable yield below the O K core level, data for CO/W(110), which was corrected for variations in incident-electron-beam current and background by x rays, shows a much smaller yield below the O K level.[59] This difference may arise from the different geometries of these surfaces, or reflect the importance of electron-beam variations and background. The ESD O^+ yield for CO/Ru below the O K level also appears to be substantial in Fig. 5, but again the PSD data for CO/Ru indicate a very small yield due to secondary-electron effects below the core level.[10] Thus the very small secondary yield contribution below the O or N K level seems to be a general phenomenon for molecular adsorbates on metals.

Figures 5 and 6 indicate that the sharp onset of the O^+ yield does not actually occur at the O K level but around 25–35 eV above the O K level (K +25–35 eV).[15,60] Figure 6 indicates that this arises not from the simple ASD process, $1\sigma^{-1}kl \rightarrow v^{-2}$, but from the shake-plus-Auger processes:[15]

$$1\sigma^{-1}3\sigma^{-1} \rightarrow v^{-2}3\sigma^{-1}$$

or

$$1\sigma^{-1}5\sigma^{-1}6\sigma^{*} \rightarrow v^{-2}5\sigma^{-1}6\sigma^{*} .$$

The resonant charge transfer from neighboring molecules, which aborts the desorption process in the v^{-2} state as discussed in Sec. II B 2 above, does not abort the desorption process for these many-electron final states, because these $3h$ and $3h$-$1e$ shake-plus-Auger final states do not depend on the Coulomb explosion for desorption. Rather, the hole in the 3σ orbital (a strongly bonding orbital) or the electron in the $6\sigma^*$ orbital (strongly antibonding) introduces a covalent repulsive force which initiates the desorption.[15] Recent PSD data utilizing polarized light indicate the peak at K +35 eV also has a significant contribution from the $1\sigma^{-1}3\sigma^{-1}2\pi 6\sigma$ excitation leading to $3h$-$2e$ final states.[10]

Figure 6 suggests that the O^+ yield around 550 eV (K +15 eV) arises from the $1\sigma^{-1}6\sigma$ excitation.[15] The recent polarization dependent PSD yields indicate that the shake-up $1\sigma^{-1}1\pi^{-1}2\pi$ excitation also contributes in this region.[10] The near absence of the $1\sigma^{-1}2\pi$ and $1\sigma^{-1}6\sigma$ excitations in the O^+ yield in Fig. 6, and the delayed on-

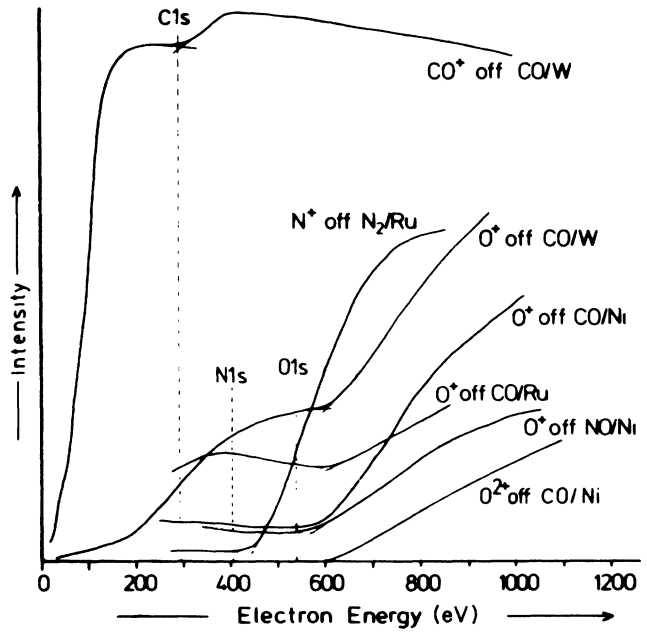

FIG. 5. Data reported by Feulner *et al.* (Ref. 58) showing the ESD ion yields from various molecular adsorbates on metal surfaces near the molecular K levels.

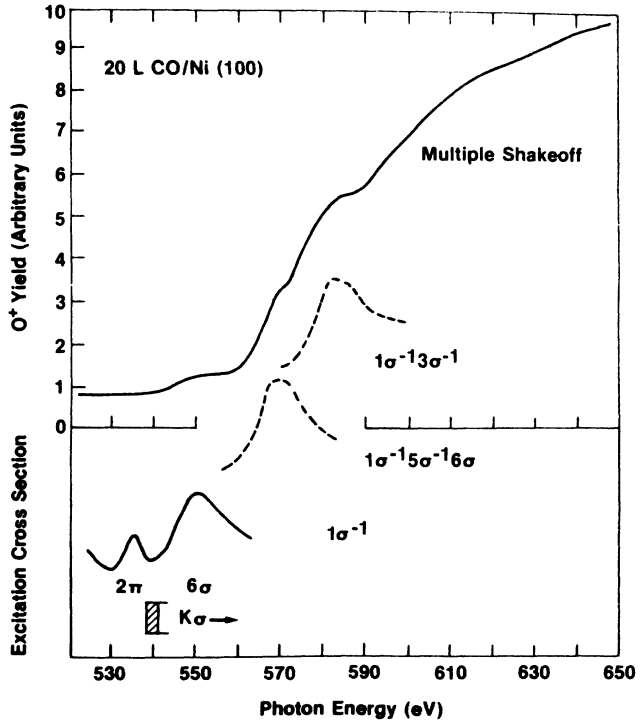

FIG. 6. Data reported by Jaeger *et al.* (Ref. 60) comparing the O^+ PSD ion yield for 20 L exposure of CO/Ni(100) with the K level excitation cross section as determined by the O KVV Auger yield. The $1\sigma^{-1}5\sigma^{-1}6\sigma$ and $1\sigma^{-1}3\sigma$ excitation cross sections are also schematically indicated as suggested by Ramaker (Ref. 15). The ion yield above 600 eV has been attributed to multiple shake-off (Ref. 15).

set in the yields in Fig. 5, clearly indicate that the simple ASD mechanism is not highly active for molecular adsorbates on metals. Obviously this arises because of charge transfer (in this case from the metal), screening the $2h$ final states and turning off the Coulomb explosion, as discussed in Sec. II B above.[15] Thus the direct ASD mechanism is essentially inactive at the core edge for the condensed gases NO and O_2 and generally all chemisorbed diatomic molecules. This means that the $1\sigma^{-1}2\pi$ and $1\sigma^{-1}6\sigma$ excitations result in desorption primarily via the indirect XESD process in both cases. On the other hand, the direct shake-plus-Auger mechanism is most certainly active in both condensed and chemisorbed diatomics. In spite of this similarity, *the $1\sigma^{-1}2\pi$ and $1\sigma^{-1}6\sigma$ excitations dominate the yield spectra for the condensed gases, but the shake-plus-Auger mechanism dominates in the chemisorbed case.*

At least three reasons can be given for the completely different relative magnitudes of the direct and indirect contributions in the condensed and chemisorbed cases. They are as follows: (a) the different magnitudes of the secondary-electron yields, (b) the different reneutralization rates, and (c) the relative efficiencies of the $2h$, $2h$-$1e$, and $3h$-$1e$ final states involved. These three points will be discussed in sequence below.

The magnitude of the secondary-electron yield in multilayer condensed gases is of course much larger than in the chemisorbed case. In the condensed gases, the secondary electrons can come from all excitations, including those far into the bulk as well as those near the surface. For the chemisorbed monolayer on the surface, only this surface layer contributes to the $1\sigma^{-1}2\pi$ and $1\sigma^{-1}6\pi$ core-level excitations. Of course, the metal can also contribute to the secondary-electron yield, but these excitations occur at different energies, generally well removed from the molecular core-level energies. Thus the XESD effect arising from the $1\sigma^{-1}2\pi$ and $1\sigma^{-1}6\pi$ excitations will be much smaller in the chemisorbed case than in the condensed case.

Because of the large free-electron density near a metal surface, one would expect that the reneutralization rate of the escaping ions would be much larger for the chemisorbed than for the condensed case. Recent ESD data indicate that almost no NO^+ and N^+ ions are observed from NO/Pt.[9] However, the N *KVV* Auger signal does decrease significantly with electron exposure.[9] This means that the N is leaving the surface as either neutral species or negative ions. The neutral species most likely result from reneutralization of the positive ion after initiation of the desorption process. The negative ions are believed to arise from the dissociative attachment process and thus begin the desorption as a negative ion.[61] This process is resonant, however, and therefore should be negligible at the 2 keV electron energies used in this work. The O^+ ions are apparently able to escape because they are further removed from the surface at initiation in the *M*-NO chemisorbed configuration. One would expect that an O^+ ion initiated from a $2h$-$1e$ final state (such as in the XESD process) would have a greater probability for reneutralization than one originating from a $3h$-$1e$ state (such as in the direct shake-plus-Auger process).

Finally, it is most interesting to compare the relative desorption efficiencies of the $2h$, $2h$-$1e$, and $3h$-$1e$ final states under various conditions. The $2h$ states (such as those in the direct ASD process) apparently become inefficient in the condensed phase for NO and O_2, and certainly also in the chemisorbed phase near the metal surface. It is well known that the valence-level PSD ion yield decreases at higher coverages, although it never goes to zero.[15,59] This is believed to arise from resonant charge transfer from neighboring molecules such as that described for the condensed phase above. It is apparent that the $2h$-$1e$ final states (such as those in the indirect XESD process) lose some of their efficiency under high coverage or in the condensed phase. The many-body $3h$-$1e$ final states (such as those produced in the direct shake-plus-Auger process) apparently remain relatively efficient in all cases as one might expect.

IV. SUMMARY

In the three systems studied for which a dominant XESD contribution has been previously postulated, we have shown that either an alternate interpretation of the data is possible (such as for NH_3/Ni), indicating that the XESD effect is small, or that the XESD process dominates only because the direct ASD mechanism is suppressed (such as for the N_2O_2 condensed gas mixture or for OH/YbO-Sm). A comparison of molecularly chemisorbed diatomic systems and condensed diatomics indicates that the relative direct and indirect yields also depend on the secondary-electron yields, the reneutralization rates, and the relative efficiencies of the various many-body final states in the desorption process. In cases for which the direct ASD process is active, the indirect XESD contribution is generally on the order of 35% or less. In chemisorbed systems, even when only the direct shake-plus-Auger process is active, the indirect XESD process is negligible. In summary, the XESD effect is generally always small. It apparently dominates the total yield only in those cases when the generally larger direct effect is suppressed.

ACKNOWLEDGMENTS

This work was supported, in part, by the U.S. Office of Naval Research. We thank the authors for use of their Figs. 1–6, particularly the authors in Ref. 2 for use of the previously unpublished Fig. 3.

APPENDIX: THEORETICAL ANALYSIS OF DATA FROM PARKS AND CO-WORKERS

As assumed by Parks *et al.*,[2] we analyze their PSD results assuming that indirect desorption is induced by secondary electrons. We further assume that all ions originate from the top surface layer, and that the surfaces are smooth and planar. We can write the direct desorption yield contributions as

$$D_{N^+}(h\nu)=[N_2]_s d_{N^+}(h\nu)\ , \tag{A1}$$

where $D_{N^+}(h\nu)$ is the direct desorption yield (ions per

photon) arising from a N 1s excitation upon photon impact with energy $h\nu$, $d_{N^+}(h\nu)$ is the N^+ ion-desorption cross section for condensed molecular N_2 upon photon impact with energy $h\nu$, and $[N_2]_s$ is the number of N_2 molecules per unit area of surface.

Similarly we have

$$D_{O^+}(h\nu)=[O_2]_s d_{O^+}(h\nu) . \quad \text{(A2)}$$

The indirect desorption yield contributions can be written

$$I^X_{Y^+}(h\nu)=[Y_2]_s \int S_X(h\nu,\varepsilon)\sigma^E_{Y^+}(\varepsilon)d\varepsilon , \quad \text{(A3)}$$

where X and Y^+ can have the combinations N and N^+, O and O^+, O and N^+, and N and O^+, $I^X_{Y^+}(h\nu)$ is the Y^+ indirect desorption yield contribution arising from a X 1s excitation upon photon impact with energy $h\nu$, $\sigma^E_{Y^+}(\varepsilon)$ is the Y^+-ion desorption cross section arising from electron impact with energy ε, $[Y_2]_s$ is the number of Y_2 molecules per unit area of surface, and $S_X(h\nu,\varepsilon)$ is the number of secondary electrons with energy ε at the surface following a X 1s excitation by a photon of energy $h\nu$.

1. Determination of the total electron yield and distribution functions

The total electron yields, following a N 1s or O 1s excitation by a photon of energy $h\nu$ can be written

$$\eta_N(h\nu)=[N_2]_b\eta^0_N(h\nu)=\int S_N(h\nu,\varepsilon)d\varepsilon , \quad \text{(A4a)}$$

$$\eta_O(h\nu)=[O_2]_b\eta^0_O(h\nu)=\int S_O(h\nu,\varepsilon)d\varepsilon , \quad \text{(A4b)}$$

where the electron yield η^0 is defined for the pure substances, N_2 or O_2, and $[N_2]_b$ or $[O_2]_b$ is the bulk concentration in the mixture relative to that in the pure substance, i.e., $[N_2]_b=0.57$ and $[O_2]_b=0.43$ for the mixtures prepared by Parks *et al.*

Let us now define the distribution functions $\rho(h\nu,\varepsilon)$ as

$$\rho_N(h\nu,\varepsilon)=S_N(h\nu,\varepsilon)/\eta_N(h\nu) \quad \text{(A5a)}$$

and

$$\rho_O(h\nu,\varepsilon)=S_O(h\nu,\varepsilon)/\eta_O(h\nu) . \quad \text{(A5b)}$$

These distribution functions can be obtained from an area-normalized energy-distribution curve (EDC) as measured in x-ray photoemission spectroscopy. Examples of such curves are indicated for graphite and gold over a range of photon energies in Fig. 7. The area under these curves before normalization reflects the total electron yield, η, as defined in Eq. (A4). In terms of ρ_X and η_X, we now have

$$I^X_{Y^+}(h\nu)=[Y_2]_s\eta_X(h\nu)\int\rho_X(h\nu,\varepsilon)\sigma^E_{Y^+}(\varepsilon)d\varepsilon . \quad \text{(A6)}$$

We can obtain several of the above quantities for N_2-O_2 (directly estimated from Fig. 3 on a relative yield scale) from the experimental data.[2] These are summarized in Table II at three different photon energies characterized by excitation into the $2\pi^*$, $6\sigma^*$, and continuum k orbitals at the N 1s and O 1s levels. We note first that $I^N_{O^+}(h\nu)/\eta_N(h\nu)$ and $I^O_{N^+}(h\nu)/\eta_O(h\nu)$ are relatively independent of $h\nu$. This is really not surprising; in fact, this I:η proportionality is the basis for some analysis of indirect mechanisms of desorption.[3] Combin-

TABLE II. Tabulation of various ion and electron yields from the mixed $[N_2]/[O_2]=1.35$:1 condensed solid as reported by Parks *et al.* (Ref. 2). The yields and ratios are defined in the text.

Yield (Arbitrary units)	400 $2\pi^*$	420 $6\sigma^*$	470 K^*	Average
$D_{N^+}+I^N_{N^+}$	1561	421	247	
$I^N_{O^+}$	142	31	17	
η_N	57	14	7	
$I^N_{O^+}/(D_{N^+}+I^N_{N^+})$	0.091	0.074	0.069	0.078
$I^N_{O^+}/\eta_N$	2.49	2.21	2.43	2.38
	530 $2\pi^*$	540 $6\sigma^*$	570 k^*	
$D_{O^+}+I^O_{O^+}$	52	37	23	
$I^O_{N^+}$	193	88	78	
η_O	22	11	7	
$I^O_{N^+}/(D_{O^+}+I^O_{O^+}$	3.71	2.38	3.39	3.16
$I^O_{N^+}/\eta_O$	8.8	8.0	11.1	9.3
	$2\pi^*$	$6\sigma^*$	k	
$\left\lvert\frac{D_{N^+}+I^N_{N^+}}{D_{O^+}+I^O_{O^+}}\right\rvert$	30	11.4	10.7	
$I^O_{N^+}/I^N_{O^+}$	1.4	2.8	4.6	

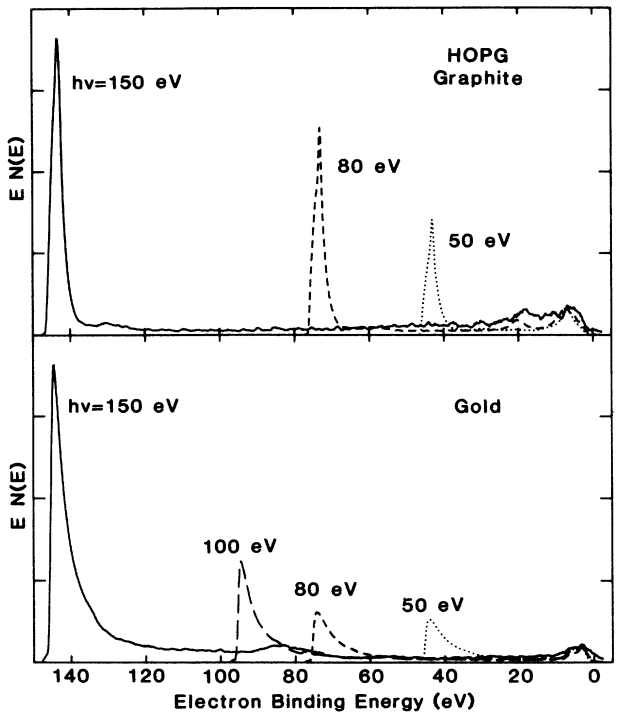

FIG. 7. Energy distribution curves obtained for highly oriented pyrolitic graphite and gold using the photon energies indicated. The curves have not been normalized so that they are representative of $S(h\nu,\varepsilon)$ as defined in Eq. (A4). These data include a correction factor for the analyzer transmission dependency on ε, so that they are indeed representative of $S(h\nu,\varepsilon)$, not $S(h\nu,\varepsilon)/\varepsilon$ as initially obtained by the retarding mode analyzer. Here $\varepsilon = h\nu -$(electron binding energy).

ing this $I:\eta$ proportionality with Eq. (A6) above, we might conclude that the expression

$$\int \rho_X(h\nu,\varepsilon)\sigma^E_{Y^+}(\varepsilon)d\varepsilon$$

is independent of $h\nu$, or further that $\rho_N(h\nu,\varepsilon)$ is independent of $h\nu$. As seen in Fig. 7, $\rho(h\nu,\varepsilon)=S(h\nu,\varepsilon)/\eta(h\nu)$ is relatively independent of $h\nu$ below $\varepsilon=25$ eV, but is very dependent on $h\nu$ at a higher ε. However, since only those electrons above the electron-stimulated desorption threshold, typically around 15–25 eV, can initiate the desorption process, only a relatively small fraction of the yield below 25 eV is of interest. Thus the $I:\eta$ proportionality can be expected only over a small energy range; i.e., narrow structural features may be similar in I and η, since narrow features in $\rho_X(h\nu,\varepsilon)$ are integrated out, but large differences in relative magnitude can occur over larger energy ranges. With these limitations in mind, we can assume that $\int \rho_X(h\nu,\varepsilon)\sigma^E_{Y^+}(\varepsilon)d\varepsilon$ is nearly independent of $h\nu$, as well as the core levels involved, so that

$$\int \rho_X(h\nu,\varepsilon)\sigma^E_{Y^+}(\varepsilon)d\varepsilon = i_{Y^+} \ . \tag{A7}$$

Equation (A6) then simplifies to

$$I^X_{Y^+}/\eta^0_X = [Y_2]_s[X_2]_b i_{Y^+} \ . \tag{A8}$$

Here the notation ignores the dependence of I and η on $h\nu$ since the ratios I/η are nearly independent of $h\nu$.

2. Determination of the direct and indirect ion yields

We can obtain expressions relating the fundamental direct and indirect ion-yield cross sections d_X and $i_X\eta_X$, as defined in Eqs. (A2) and (A8), respectively, utilizing the experimentally determined and $h\nu$-independent ratios

$$I^X_{X^+}/(D_{X^+}+I^X_{X^+})$$

and

$$I^X_{Y^+}/\eta_X \ (X=\text{N or O},\ Y^+=\text{N}^+ \text{ or } \text{O}^+)$$

in Table II. We obtain the following:

$$\frac{I^N_{O^+}}{D_{N^+}+I^N_{N^+}}\frac{I^O_{N^+}}{\eta_O}\frac{\eta_N}{I^N_{O^+}} = \frac{i_N\eta_N}{d_N+i_N\eta_N} = 0.30 \tag{A9a}$$

and

$$\frac{I^O_{N^+}}{D_{O^+}+I^O_{O^+}}\frac{I^N_{O^+}}{\eta_N}\frac{\eta_O}{I^O_{N^+}} = \frac{i_O\eta_O}{d_O+i_O\eta_O} = 0.81 \ , \tag{A9b}$$

which relates the indirect XESD cross section to the total. Rearranging these equations gives

$$\frac{d_N}{i_N\eta_N} = 2.3 \ , \tag{A10a}$$

$$\frac{d_O}{i_O\eta_O} = 0.24 \ , \tag{A10b}$$

which relates the direct to the indirect XESD cross sections. Equation (A9) above indicates that the indirect XESD channel has a 30% effect for N^+ desorption (N^+ yield at the N^+ core level), but dominates the O^+ desorption (O^+ yield at the O^+ core level) at 81% of the total for the mixed 1.35:1 N_2-O_2 condensed solid. The XESD effect will be even larger in the pure solids since using Eqs. (A4), and (A9), and (A10), we obtain $d_N/i_N\eta^0_N = 1.3$ and $d_O/i_O\eta^0_N = 0.10$, giving a 43% XESD effect for N^+ desorption from pure N_2 and a 91% effect for O^+ from pure O_2.

The calculation for the pure solids assumed that d_X and i_X are the same in the pure and mixed solids, so that only the bulk concentration introduced in Eq. (A4) has an effect on the change in the XESD effect for the pure and mixed solids. Although this approximation is a reasonable one, considering the weak intermolecular interactions in these van der Waals solids, we indicate above that d_X, in fact, may be reduced substantially in the mixed solid, but sufficient evidence exists (also discussed above) indicating that the XESD process dominates even for the pure O_2 solid.

The 30–40% XESD effect for N_2 is comparable to that found previously for H^+ desorption from OH/TiO_2,[12] and thus is very reasonable. The dramatic increase in relative magnitude of the XESD effect for O_2 could have two possible causes: either (1) i_O is extremely large for O_2, or (2) d_O is extremely small. We can show that the latter is true by comparing the ratios $(D_{N^+}+I^N_{N^+})/(D_{O^+}+I^O_{O^+})$ for the mixture, given in

Table II, to that for the pure solids as reported by Rosenberg *et al.*[26] and given in Table I. This ratio, of course, depends on two different $h\nu$ energies, namely that in the region of the N and O K levels. In Table II we show that this ratio is relatively constant for excitation into the $6\sigma^*$ and k continuum above each core level. The reason why it is very different for excitation into the $2\pi^*$ level is due to the different decay mechanisms possible upon excitation into the $2\pi^*$ bond level as explained in Sec. II B 2. The ratio involving two widely different photon energies also require a knowledge of the relative photon fluxes in the O K and N K regions. Parks *et al.* indicate that for their synchrotron source and monochromator settings the photon fluxes differed by a factor of almost 2 (i.e., $f_N/f_O \sim 1.9$). Rosenberg reports absolute cross sections, so that the relative photon fluxes have already been corrected for in his data. Rosenberg reports yields on the pure substances only for excitation into the 6σ level, so we will use this excitation for the mixture as well as the pure solids. Thus we have

$$\frac{f_O}{f_N}\frac{D_{N^+}+{}^N I_{N^+}}{D_{O^+}+{}^O I_{O^+}}=\frac{[N_2]_s}{[O_2]_s}\frac{d_N+\eta_N^0[N_2]_b i_N}{d_O+\eta_O^0[O_2]_b i_O}$$

$$=6.0 \quad \text{(for the mixture)} \qquad \text{(A11a)}$$

and

$$\frac{D_{N^+}+I_{N^+}^N}{D_{O^+}+I_{O^+}^O}=\frac{d_N+\eta_N^0 i_N}{d_O+\eta_O^0 i_O}=3.1 \quad \text{(for the pure solids)}\,, \qquad \text{(A11b)}$$

where we have assumed $[N_2]_s/[O_2]_s=1$ for the pure solids and again that d_X and i_X are the same in the pure and mixed solids. From Eqs. (A10) and (A11b), we obtain $d_N/d_O=20$, which can be inserted into Eq. (A11a) to give $[N_2]_s/[O_2]_s=1.1$. Furthermore, we obtain from Eq. (A10)

$$\frac{i_N\eta_N}{i_O\eta_O}=\frac{0.24}{2.3}20=2.1\,,$$

or from the corresponding equation involving η_X^0,

$$\frac{i_N\eta_N^0}{i_O\eta_O^0}=\frac{0.10}{1.3}20=1.5\,.$$

Thus the indirect XESD cross sections for N and O differ by only a factor of 2, but the direct cross sections differ by a factor of 20. Note also from Table II that at the $1s\rightarrow 6\sigma^*$ excitation $\eta_O^0/\eta_N^0=\frac{11}{14}\times 1.35=1.06$, so that the secondary-electron yields for the pure substances are nearly equal. The $[N_2]_s/[O_2]_s$ ratio indicates that to within experimental uncertainty the surface and bulk concentrations ($[N_2]_b/[O_2]_b=1.35$) are comparable.

[1]R. Jaeger and J. Stöhr, Phys. Rev. B **28**, 1145 (1983); R. Jaeger, J. Stöhr, and T. Kendelewicz, Surf. Sci. **134**, 547 (1983).

[2](a) C. C. Parks, Lawrence Berkeley Laboratory Report No. LBL-16892, 1983 (unpublished); (b) V. Rehn and R. A. Rosenberg, in *Synchrotron Radiation Research: Advances in Surface and Low-Dimensional Science,* edited by R. Z. Bachrach (Plenum, New York, 1987); (c) R. A. Rosenberg, V. Rehn, and C. C. Parks (unpublished).

[3]J. Schmidt-May, F. Senf, J. Voss, C. Kunz, A. Flodström, R. Nyholm, and R. Stockbauer, in *Desorption Induced by Electronic Transitions,* Vol. 4, of *Springer Series in Surface Sciences,* edited by W. Brenig and D. Menzel (Springer-Verlag, Heidelberg, 1984), p. 94; Surf. Sci. **163**, 303 (1985).

[4]E. Bertel, R. Stockbauer, D. E. Ramaker, and T. E. Madey, Phys. Rev. B **31**, 5580 (1985).

[5]T. E. Madey, R. Stockbauer, J. F. van der Veen, and D. E. Eastman, Phys. Rev. Lett. **45**, 187 (1980).

[6]R. L. Benbow, M. R. Thuler, and Z. Hurych, Phys. Rev. Lett. **49**, 1264 (1982).

[7]D. E. Ramaker, E. Bertel, R. L. Kurtz, R. Stockbauer, and T. E. Madey, Phys. Rev. B **31**, 6840 (1985).

[8]R. A. Rosenberg, P. J. Love, V. Rehn, I. Owen, and G. Thornton, J. Vac. Sci. Technol. A **4**, 1451 (1986).

[9]U. Schwalke, H. Niehus, and G. Comsa, Surf. Sci. **137**, 23 (1984).

[10]R. Treichler, W. Riedl, W. Wurth, P. Feulner, and D. Menzel, Phys. Rev. Lett. **54**, 462 (1985).

[11]B. B. Pate, M. H. Hecht, C. Binns, I. Lindau, and W. E. Spicer, J. Vac. Sci. Technol. **21**, 364 (1982).

[12]F. L. Hutson, D. E. Ramaker, V. M. Bermudez, and M. A. Hoffbauer, J. Vac. Sci. Technol. A **3**, 1657 (1985).

[13]D. E. Ramaker, *Desorption Induced by Electronic Transitions,* edited by N. H. Tolk, M. M. Traum, J. C. Tully, and T. E. Madey (Springer, Berlin, 1982), p. 70.

[14]T. E. Madey, D. E. Ramaker, and R. Stockbauer, Annu. Rev. Phys. Chem. **35**, 215 (1984).

[15]D. E. Ramaker, J. Chem. Phys. **78**, 2998 (1983).

[16]C. C. Parks, D. A. Shirley, M. L. Knotek, G. Loubriel, R. H. Stulen, B. E. Koel, and R. A. Rosenberg (unpublished).

[17](a) R. Jaeger, J. Stöhr, J. Feldhaus, S. Brennan, and D. Menzel, Phys. Rev. B **23**, 2101 (1981). (b) R. E. Honig and H. O. Hook, RCA Rev. **21**, 360 (1960).

[18]T. E. Madey and C. Benndorf, Surf. Sci. **152/153**, 587 (1985); C. Benndorf and T. E. Madey, *ibid.* **135**, 164 (1983); F. P. Netzer and T. E. Madey, *ibid.* **119**, 422 (1982).

[19]R. L. Kurtz, N. Usuki, R. Stockbauer, and T. E. Madey, J. Electron Spectrosc. Relat. Phenom. **40**, 35 (1986).

[20]R. A. Rosenberg, V. Rehn, A. K. Green, P. R. Laroe, and C. C. Parks, *Desorption Induced by Electronic Transitions,* edited by N. H. Tolk, M. M. Traum, J. C. Tully, and T. E. Madey (Springer, Berlin, 1982), p. 247.

[21]D. E. Ramaker, Chem. Phys. **80**, 183 (1983).

[22]T. A. Carlson and M. O. Krause, J. Chem. Phys. **56**, 3206 (1972).

[23]H. Petersen, A. Bianconi, F. C. Brown, and R. Z. Bachrach, Chem. Phys. Lett. **58**, 263 (1978).

[24]R. E. LaVilla, J. Chem. Phys. **63**, 2733 (1975).

[25]D. M. Barrus, R. L. Blake, A. J. Burek, K. C. Chambers, and A. L. Pregenzer, Phys. Rev. A **20**, 1045 (1975).

[26]R. A. Rosenberg, P. J. Love, P. R. Laroe, V. Rehn, and C. C.

Parks, Phys. Rev. B **31**, 2634 (1985).
[27]B. Brehm and G. de Frenes, Int. J. Mass Spectrom. Ion Phys. **26**, 251 (1978).
[28]A. R. Miedema, Z. Metallkd. **69**, 455 (1978); **69**, 287 (1978).
[29]A. R. Miedema and R. Boom, Z. Metallkd. **69**, 183 (1978).
[30]P. W. Atkins, *Physical Chemistry* (Freeman, San Francisco, 1978), p. 112.
[31]*Handbook of Chemistry and Physics* (Chemical Rubber, Cleveland, 1984).
[32]P. L. Kronebusch and J. Berkowitz, Int. J. Mass Spectrom. Ion Phys. **22**, 283 (1976).
[33]M. Nakamura, Y. Morioka, S. Aoyama, Y. Kageyama, T. Hayaishi, I. H. Suzuki, G. Isoymama, S. Asaoka, and E. Ishiguro, Ann. Isr. Phys. Soc. **6**, 229 (1984).
[34]J. A. R. Samson, J. L. Gardner, and G. N. Haddad, J. Electron Spectros. Relat. Phenom. **12**, 281 (1977).
[35]M. Richard-Viard, O. Dutuit, M. Lavollee, T. Govers, P. M. Guyon, and J. Durup, J. Chem. Phys. **82**, 4054 (1985).
[36]J. A. Nichols, D. L. Yeager, and P. Jorgensen, J. Chem. Phys. **80**, 293 (1984).
[37]J. Goodman and L. E. Brus, J. Chem. Phys. **67**, 4398 (1977); **67**, 4408 (1977).
[38]C. S. Barrett, L. Meyer, and J. Wasserman, J. Chem. Phys. **47**, 592 (1967).
[39]R. J. Meier and R. B. Helmholdt, Phys. Rev. B **29**, 1387 (1984).
[40]L. Meyer, in *Advances in Chemical Physics,* edited by I. Prigogine and S. A. Rice (Wiley, New York, 1970), Vol. 26, p. 343.
[41]Y. B. Gaididei, V. M. Loktev, V. S. Ostrovskii, and A. F. Prikhotko, Dok. Akad. Nauk, SSSR **272**, 62 (1983) [Sov. Phys.—Dokl. **28**, 738 (1983)]; Y. B. Gaididei, V. M. Loktev, A. F. Prikhotko, and L. I. Shanskii, Phys. Status Solidi **72**, 795 (1975); **73**, 415 (1976).
[42]Y. G. Litvinenko, V. V. Eremenko, and T. I. Garber, Phys. Status Solidi **30**, 49 (1968).
[43]H. J. Lau, J. H. Fock, and E. E. Koch, Chem. Phys. Lett. **89**, 281 (1982).
[44]J. H. Fock and E. E. Koch, Ann. Isr. Phys. Soc. **6**, 285 (1984).
[45]B. B. Tonner, C. M. Kao, E. W. Plummer, T. C. Caves, R. P. Messmer, and W. R. Salaneck, Phys. Rev. Lett. **51**, 1378 (1983).
[46]C. M. Kao, T. C. Caves, and R. P. Messmer, J. Vac. Sci. Technol. A **2**, 922 (1984).
[47]L. Sanche and M. Michaud, J. Chem. Phys. **81**, 257 (1984).
[48]H. Nakatsuji, Chem. Phys. **75**, 425 (1983).
[49]W. Domcke, L. S. Cederbaum, J. Schirmer, W. von Niessen, C. E. Brion, and K. H. Tan, Chem. Phys. **40**, 171 (1979).
[50]L. Pettersson, M. Backstrom, R. Brammer, N. Wassdahl, J. E. Rubensson, and J. Nordgren, J. Phys. B **17**, L279 (1984).
[51]D. A. Morales and G. E. Ewing, Chem. Phys. **53**, 141 (1980).
[52]T. E. Gough, R. F. Miller, and G. Scoles, J. Chem. Phys. **69**, 1588 (1978).
[53]H. Abe and R. Onaka, J. Phys. Soc. Jpn. **53**, 1176 (1984).
[54]J. H. Fock, H. J. Lau, and E. E. Koch, Ann. Isr. Phys. Soc. **6**, 191 (1984).
[55]A. P. Hitchcock, C. E. Brion, and M. J. van der Wiel, Chem. Phys. Lett. **66**, 213 (1979).
[56]R. Locht, G. Caprace, and J. Momigny, Chem. Phys. Lett. **111**, 560 (1984).
[57]J. L. Olivier, R. Locht, and J. Momigny, Chem. Phys. **84**, 295 (1984); **68**, 201 (1982).
[58]P. Feulner, R. Triechler, and D. Menzel, Phys. Rev. B **24**, 7427 (1981).
[59]J. E. Houston and T. E. Madey, Phys. Rev. B **26**, 554 (1982).
[60]R. Jaeger, J. Stöhr, R. Treichler, and L. Baberscke, Phys. Rev. Lett. **47**, 1300 (1981); R. Jaeger, R. Treichler, and J. Stöhr, Surf. Sci. **117**, 533 (1982).
[61]D. E. Ramaker, in *Desorption Induced by Electronic Transitions,* Vol. 4 of *Springer Series in Surface Science,* edited by W. Brenig and D. Menzel (Springer, Heidelberg, 1985), p. 10.